Sensitivity of the jet quenching observables to the temperature dependence of the energy loss

Francesco Scardina,[1,3,*] Massimo Di Toro,[2,3] and Vincenzo Greco[2,3,†]
[1]*Department of Physics, University of Messina, I-98166 Messina, Italy*
[2]*Department of Physics and Astronomy, University of Catania, Via S. Sofia 64, I-95125 Catania, Italy*
[3]*INFN-Laboratori Nazionali del Sud, Via S. Sofia 62, I-95125 Catania, Italy*
(Received 7 September 2010; published 1 November 2010)

The quenching of minijets (particles with $p_T \gg T, \Lambda_{\rm QCD}$) in ultrarelativistic heavy-ion collisions has been one of the main predictions and discoveries at the BNL Relativistic Heavy Ion Collider. We analyze the correlation between different observables like the nuclear modification factor $R_{AA}(p_T)$, the elliptic flow, and the ratio of quark to gluon suppressions. We show that the temperature (or entropy density) dependence of the in-medium energy loss strongly affects the relation among these observables. In particular, the large elliptic flow and the nearly equal $R_{AA}(p_T)$ of quarks and gluons can be accounted for only if the energy loss occurs mainly around T_c and the $q \leftrightarrow g$ conversion is significant. The use of an equation of state fitted to lattice QCD calculations, slowing down the cooling as $T \to T_c$, seems to contribute to both the enhancement of v_2 and the efficiency of the conversion mechanism.

DOI: 10.1103/PhysRevC.82.054901 PACS number(s): 12.38.Mh, 25.75.Ld

The experiments at the BNL Relativistic Heavy Ion Collider (RHIC) are dedicated to studying the properties of the matter at exceedingly high density and temperature. Under such extreme conditions, the matter was expected to undergo a deconfinement and chiral phase transition and have quarks and gluons as degrees of freedom. The theoretical and experimental efforts have shown that, indeed, a new form of matter has been created [1]. Such a matter appears as a nearly perfect fluid with very low viscosity to entropy density [2,3]. It develops strong collective modes with quarks as degrees of freedom and hadronizes in a modified way with respect to pp collisions, at least in the intermediate $2 \leqslant p_T \leqslant 5$-GeV region [4,5]. One way to probe the created matter is to exploit the high-energy jets ($p_T \gg T, \Lambda_{\rm QCD}$) produced by the hard collisions at the initial stage. They are internal probes propagating through the fireball and interacting with the medium, hence carrying information on its properties, as proposed long ago in Refs. [6–8]. It has indeed been shown that the matter has a very high opacity with respect to high-p_T partons that traverse the hot medium in agreement with the expectations about the energy loss in QCD medium [8–10]. This energy loss can be quantified by the suppression of observed hadron spectra at high transverse momenta p_T, as well as in the suppression of back-to-back dihadron correlations with a high-p_T trigger, when compared with pp or dA collisions [1,11]. Both these phenomena related to the "jet quenching" have been observed and represent one of the major discoveries of the RHIC experimental program [1].

However, even if the observation of the jet suppression cannot be questioned, there are several fundamental questions that still remain open. There are indeed several models that depend in a different way on temperature T [12,13] or that do not depend explicitly on T but on the $\hat{q}$ transport coefficient [14,15]; some others are based on perturbative approach and others on higher twist expansion [16,17].

Despite differences, all of the approaches seem to be able to describe the amount of suppression $R_{AA}(p_T)$ observed experimentally. It is evident that one needs to go one or two steps further and, fortunately, experimentally, there are already other observables related to the jet quenching phenomena available. Interestingly, the present models do not seem to be able to account for all of them simultaneously. In this article we focus on two observables beyond the $R_{AA}(p_T)$. One is the elliptic flow $v_2(p_T)$ and the other is the flavor dependence of the suppression that we mainly discuss in terms of $R_{AA}(q)/R_{AA}(g)$. The latter can be experimentally inferred by a systematic comparison of the different suppression for π, ρ, K, p, and $\bar{p}$, which are differently related to quark and gluon suppression.

The purpose of the present article is to show that the jet quenching mechanism carries much more information than can be inferred from only the nuclear modification factor $R_{AA}(p_T)$ and even the jet-triggered angular information. We suggest that the study of the correlation between the elliptic flow v_2 and the flavor dependence of the quenching $R_{AA}(q)/R_{AA}(g)$ is rich in information on the temperature dependence of the quenching and on the mechanism of parton flavor conversion.

We point out that a correlation between v_2 and $R_{AA}(q)/R_{AA}(g)$ is sensitive to the temperature (or entropy density s) dependence of $\Delta E_{\rm loss}$ and on the density profile of the bulk. The latter becomes unexpectedly dramatic if an extreme T, ρ, or s dependence is considered as in the recent works of J. Liao and E. Shuryak [18] or V. S. Pantuev [19]. This shows, in general, that once one goes beyond the $R_{AA}(p_T)$ a more careful treatment of the time evolution of the fireball becomes mandatory, but also the simultaneous description of $R_{AA}(p_T)$, v_2, and $R_{AA}(q)/R_{AA}(g)$ [or the ratio of the $R_{AA}(p_T)$ between different hadrons] is nontrivial and more rich in information. In particular we find that the energy loss increasing as $T \to T_c$, the $q \leftrightarrow g$ in-medium conversion and the expansion-cooling of the fireball according to a lattice

*scardinaf@lns.infn.it
†greco@lns.infn.it

QCD EoS all go in the direction of improving the agreement with the three observables.

The article is organized in five sections. In Sec. I the main ingredients of the model are presented. In Sec. II the model is applied to calculate the $R_{AA}(p_T)$ as a function of momentum and centrality. In Sec. III the elliptic flow and the ratio of quark to gluon $R_{AA}(p_T)$ are discussed together with their correlation. In Sec. IV the impact of a realistic EoS is presented. In the last section we summarize the conclusions from the present study.

I. MODELING THE JET QUENCHING

Our modeling of the jet energy loss is based on the very widely used adiabaticlike approximation for which the jet loses energy in a bulk medium that is independently expanding and cooling. Therefore, the jet energy loss is considered to be a small perturbation of the bulk dynamics. This essentially has been the main assumption in the model until now, even if the higher energy at CERN Large Hadron Collider (LHC) should make this assumption inadequate owing to the significant amount of energy that is contained in the high-p_T partons initially produced.

The main components of our model can be easily sketched in the following way.

A. Initial conditions

The parton distributions are calculated in the next-to-leading-order perturbative QCD (pQCD) scheme: They are parametrized by power-law functions as

$$\frac{dN_f}{d^2p_T} = \frac{A_f}{(1 + p_T/B_f)^{n_f}}, \tag{1}$$

with $f = q, \bar{q}, g$. The transverse momentum p_T is in units of GeV and the values of the parameters A_f, B_f, and n_f are given in Table I and are taken from Ref. [20]. Such a choice is driven mainly by the intention to make a direct contact and comparison with the several works discussing jet quenching with the flavor conversion [20–24].

As regards the parton distribution in space coordinates, it scales with the number of binary nucleon collision $N_{\rm coll}$ according to the standard Glauber model [25,26]. The initial conditions for the bulk medium are described by the density profile $\rho(\vec{r}, z, \tau)$ that in the longitudinal direction evolves according to the Bjorken expansion at the velocity of light. The initial transverse density profile is instead proportional to the standard Glauber model participant distribution:

$$\rho_{\rm part}(\vec{b}, \vec{r}) = t_A(\vec{r})[1 - e^{-\sigma_{NN} t_A(\vec{b}-\vec{r})}] + t_B(\vec{b} - \vec{r})[1 - e^{-\sigma_{NN} t_A(\vec{r})}], \tag{2}$$

TABLE I. Parameters for initial parton minijet distribution given in Eq. (1) at midrapidity for Au + Au at $\sqrt{s_{NN}} = 200$ A GeV. Taken from Ref. [20].

	A_f (GeV)	B_f (GeV)	n_f
g	1440	1.5	8.0
q	670	1.6	7.9
$\bar{q}$	190	1.9	8.9

with $\sigma_{NN} = 42$ mb, $\vec{b}$ the impact parameter vector, and t_A the nuclear thickness function normalized to the number of nucleons and given by

$$t_A(\vec{r}) = \int_{-\infty}^{+\infty} dz \rho_A(\vec{r}, z), \tag{3}$$

where $\rho_A(\vec{r})$ is the nuclear density that we have taken to be a Woods-Saxon (WS) with radius $R = 6.38$ fm and thickness $a = 0.535$ fm. The total number of participants is therefore

$$N_{\rm part}(b) = \int d^2r \rho_{\rm part}(b, \vec{r}). \tag{4}$$

Beyond the Glauber density profile we have also considered a simplified sharp elliptic (SE) shape with the $\vec{x}$ and $\vec{y}$ axis adjusted to reproduce the same eccentricity of the Glauber model at each impact parameter. The SE shape has been used for the description of the bulk in several jet quenching models [20–22,27].

B. Bulk density evolution

For the SE shape the density space-time evolution is given by

$$\rho(x, y, \tau) = \frac{1}{\tau A_T(\tau)} \frac{dN}{dy_z} \Theta\left(1 - \frac{x^2}{R_x^2(\tau)} - \frac{y^2}{R_y^2(\tau)}\right), \tag{5}$$

where $A_T = \pi R_x^2 R_y^2$ is the transverse area of the evolving fireball and R_x, R_y are the lengths of the two axes of the ellipse. These can in general evolve according to an expansion at constant acceleration or constant velocity,

$$\begin{aligned} R_x(\tau) &= R_{xo} + v_T\tau + \tfrac{1}{2}(a_T + \epsilon_a)\tau^2, \\ R_y(\tau) &= R_{yo} + v_T\tau + \tfrac{1}{2}(a_T - \epsilon_a)\tau^2, \end{aligned} \tag{6}$$

with v_T the transverse velocity and $a_T \pm \epsilon_a$ the acceleration that through ϵ_a can be taken to be different between the x and y directions to simulate the anisotropic azimuthal expansion that reduces the eccentricity with time. We have used a typical value of $a_T = 0.08$ fm^{-1} that generates a final radial flow $\beta = 0.4$, with $v_T = 0$, $\epsilon_a = 0.04$ fm^{-1}, with a slight dependence on the impact parameter of the collision. However, the sensitivity of the jet quenching on these parameters is quite limited.

For the case with the Glauber profile the evolution of the local density is similarly given by

$$\rho(x, y, \tau) = \frac{1}{\tau A_T(\tau)} \frac{dN}{dy} P_{\rm eff}(x, y, \tau), \tag{7}$$

where with respect to Eq. (5) the θ function is substituted by the profile function $P_{\rm eff}(x, y, \tau)$ and A_T is now the effective area given by the space integral of the profile function,

$$\begin{aligned} P_{\rm eff}(x, y, \tau) &= \frac{N_{\rm part}(x, y, \tau)}{N_{\rm part}(0, 0, \tau)}, \\ A_T &= \iint dx dy P_{\rm eff}(x, y, \tau), \end{aligned} \tag{8}$$

where $N_{\rm part}(x, y, \tau_0)$ is given by the Glauber model while the time dependence is determined by the expansion in the x-y plane according to Eq. (6).

C. Energy loss

The aim of our work is to explore the consequences of different T dependencies of energy loss on the observables; hence, we employ various schemes for the energy loss. However, to make a connection to the large amount of effort to evaluate gluon radiation in a pQCD frame we will use also the Gyulassy-Levai-Vitev (GLV) formula at first order in the opacity expansion [10,27],

$$\frac{\Delta E(\rho,\tau,\mu)}{\Delta\tau} = \frac{9\pi}{4} C_R \alpha_s^3 \rho(x,y,\tau)\tau \log\left(\frac{2E}{\mu^2\tau}\right), \quad (9)$$

where C_R is the Casimir factor equal to $4/3$ for quarks and 3 for gluons, $\mu = gT$ is the screening mass with $g = 3$ in agreement with lattice QCD (lQCD) results [28] and τ is the time minus the initial time $\tau_i = 0.2$ fm. Furthemore, considering massless partons at midrapidity $E = p_T$. There are corrections to Eq. (9) coming from higher order that can be approximately accounted for by a rescaling the Z factor of the energy loss. However, this is not really relevant for the objectives of the present work because we renormalize the energy loss to have the observed amount of suppression $R_{AA}(p_T)$ for central collisions (see next section). In fact, our purpose is to study how other variables can change once $R_{AA}(p_T)$ has been fixed to experimental data for central collisions.

Usually in the GLV, as well as in other approaches, the temperature evolution of the strong coupling α_s is discarded. We consider the impact of such a dependence to understand the amount of T dependence that can come simply from the asymptotic freedom in a pQCD approach. The scale dependence of the strong coupling can be written as

$$\alpha_s(Q^2) = \frac{4\pi}{\beta_0 \ln\left(-Q^2/\Lambda^2_{\rm QCD}\right)}, \quad (10)$$

where $\beta_0 = 11 - \frac{2}{3}N_f$ and the thermal scale $Q^2 = 2\pi T^2$, which makes it possible to get a correct behavior of the screening mass μ on the energy scale [28].

In Fig. 1 we show using dot-dashed and dashed lines the temperature dependence of the energy loss for the GLV with a dependence of the coupling according to Eq. (10) [GLV-$\alpha_s(T)$] and with a constant coupling $\alpha_s = 0.27$ (GLVc). In itself the effect of the asymptotic freedom that reduces α_s at an increasing energy scale significantly modifies the temperature dependence of the energy loss. However, we see that such effect is not very large once the coupling itself is readjusted to produce the correct amount of suppression.

In Fig. 1 we have also shown two other opposite cases for $\Delta E/\Delta\tau$: the thick line that shifts the energy loss to lower temperature (hence low-density ρ or entropy density s) as suggested in [18,19] and the thin line that gives a dominance of quenching at high T, considered here just for comparison with respect to the opposite case. For both $E_{\rm loss}$ we have a standard dependence on the transverse momentum, $\Delta E(p_T) \sim p_T^\gamma$ with $\gamma = 0.6$.

We have plotted in Fig. 1 the $\Delta E_{\rm loss}$ as a function of the temperature; however, under the hypothesis of local equilibrium for the bulk this is equivalent to a density or an entropy-density dependence used by other authors. In the model implemented, we generally employ the free gas

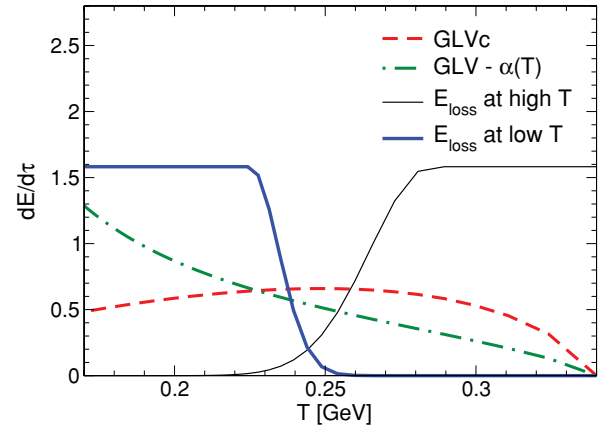

FIG. 1. (Color online) Temperature dependence of the energy loss for a parton at $p_T = 10$ GeV. The dashed and dot-dashed lines represent the GLV energy loss with constant and T-dependent α_s coupling, respectively (see text). The thick line is the case in which the energy loss take place only closer to the phase transition, and the thin line represents an opposite case in which the energy loss takes place only at high T.

approximation to relate density, temperature, and time. As is well known, one has

$$\rho = \frac{\zeta(3)}{\pi^2}\left(\frac{3}{4}d_{q,\bar{q}} + d_g\right) T^3 \to 4.2T^3, \quad (11)$$

where the last expression is obtained with $d_{q,\bar{q}} = 24$, $d_g = 16$. From Eq. (11) with an initial temperature $T_0 = 340$ MeV at $\tau_0 = 0.6$ fm and a transverse area $A_T \sim 90$ fm^2, one has a $dN/dy \sim 1000$ for $b = 3$ fm corresponding to 0%–10%, in agreement with standard estimates. Equation (11) allows one to evaluate the local temperature from the local density given by Eq. (5) for the SE profile and by Eq. (7) for the Glauber WS profile. For a one-dimensional (1D) Bjorken expansion and the SE profile, Eq. (11) gives a direct correlation between density ρ, temperature T, and time τ,

$$\frac{T}{T_0} = \left(\frac{\rho}{\rho_0}\right)^{1/3} = \left(\frac{\tau_0}{\tau}\right)^{1/3}, \quad (12)$$

with T_0, ρ_0, and τ_0 the values at same initial time. By means of Eq. (12) we can relate the $\Delta E/\Delta\tau$ represented by the thick solid line in Fig. 1 to the delayed energy loss employed by Pantuev [19]. In particular with our parameters from Eq. (12), our thick solid line corresponds to a delay of about 1.8 fm close and even less extreme than the one in Ref. [19]. One can also notice that for some observables already the less extreme GLV-$\alpha_s(T)$ can give results similar to the low-T energy loss (see Figs. 5 and 8).

D. Hadronization

The final step of the model is the hadronization by independent fragmentation. The parton distribution after the jet quenching are employed to evaluate the hadron spectrum by independent jet fragmentation using the Albino-Kramer-Kniehl (AKK) fragmentation functions $D_f^H(x, Q^2)$, which

give the probability that a hadron H is formed from a parton of flavor f. The final hadronic spectrum is obtained from

$$\frac{dN_H}{d^2p_T} = \int_0^1 dx x \sum_f \frac{dN_f}{d^2p_T} D_f^H(x, Q^2), \tag{13}$$

where $x = p_T^H/p_T^f$ is the fraction of the f parton carried by the hadron H and $Q = p_T^f/2$ is the energy scale. At RHIC there have been several evidences that while hadronization by independent fragmentation is able to describe proton-proton spectra at $p_T \geqslant 2$ GeV, in Au + Au collisions there are nonperturbative effects like quark coalescence that modify hadronization at least up to $p_T \sim 5$–6 GeV [4,5]. We do not include any hadronization by coalescence in the present work; therefore, all of the following results have to be considered reliable only for $p_T \geqslant 5$ GeV.

II. APPLICATION OF THE MODEL TO EVALUATE $R_{AA}(p_T)$

The amount of quenching is quantified by comparison of the inclusive spectra $d^2N^{AA}/dp_t d\eta$ in ion-ion (AA) collision to a nucleon-nucleon (pp) reference $d^2\sigma^{NN}/dp_t d\eta$ via the nuclear modification factor $R_{AA}(p_t)$,

$$R_{AA}(p_t) \equiv \frac{d^2N^{AA}/dp_t d\eta}{T_{AA} d^2\sigma^{NN}/dp_t d\eta}, \tag{14}$$

with T_{AA} the nuclear overlap function that scales up a single NN cross section to AA according to expected number of binary NN collisions *without* modification. Thus, a R_{AA} smaller (larger) than unity means suppression (enhancement) owing to medium effect. At RHIC this ratio at large $p_t >$ 6 GeV has been measured to be nearly constant around a value of 0.2 for the most central Au + Au collisions, see Fig. 2 (top). In our model the $R_{AA}(p_T)$ can be calculated simply from the ratio of the spectra before and after quenching.

We have applied our modeling of the jet quenching for Au + Au collisions at 200 AGeV. We use standard initial conditions that for the most central collision bin, $b = 3$ fm, are given by a $dN/dy = 1000$ and a maximum temperature of the bulk $T_0 = 340$ MeV at $\tau_0 = 0.6$ fm, as usually done to describe the bulk in hydrodynamics and transport approaches [29,30]. The results are shown in Fig. 2 and are performed for the two geometries described previously: WS profile and SE shape. The GLV formula [Eq. (9)] is used with a coupling $\alpha_s = 0.27$ but rescaled by a $Z = 0.45$ factor [31] that accounts for higher-order effect. Here it has been chosen to reproduce the data at $p_T = 6$ GeV for the most central selection 0%–5%. From the WS profile to the SE, one has to decrease by about 15% the Z normalization factor owing to lack of surface where the quenching is smaller. However, both values are well inside the uncertainty in the α_s strength of the in-medium gluon radiation owing to the uncertainty in the perturbative expansion and in the validity of the expansion itself. However, as said in the Introduction our purpose is not to constrain the total amount of quenching owing to gluon radiation. Our methodology is to fit the $R_{AA}(p_T)$ to fix the correct amount of total quenching with the aim of exploring the effect of different geometries and especially different temperature (ρ or s) dependencies of the energy loss on other observables.

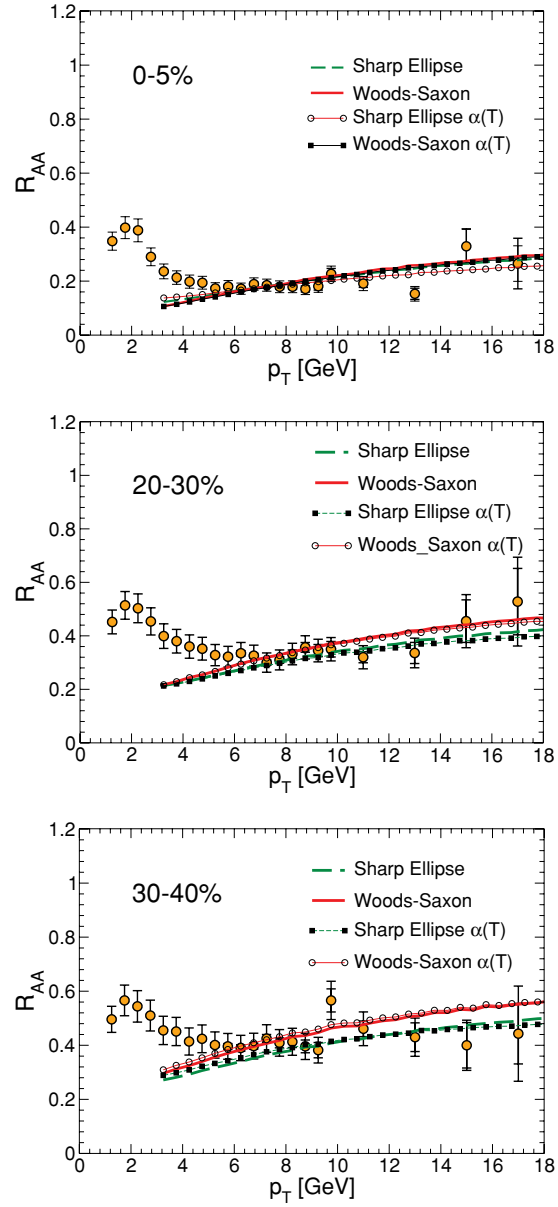

FIG. 2. (Color online) Nuclear modification factor as a function of the transverse momentum p_T in Au + Au at 200 A GeV for different centralities. The circles are the experimental data taken from Ref. [11]. The calculations using the GLV energy loss are shown by the dashed and solid lines for a SE profile and a WS profile, respectively. The squares and open circles refer to GLV-$\alpha_s(T)$ for a SE and WS profiles, respectively.

In Fig. 2 we can see that once the amount of quenching is fixed for the most central collisions, the dependence on both p_T and centrality are correctly predicted with a GLV formula for quenching. Of course, such a result has been obtained with other models of gluon radiation like Baier-Dokshitzer-Mueller-Peigne-Schiff, Armesto-Salgado Wiedemann, Arnold-Moore-Yaffe,

Djordjevic-Gyulassy-Levai-Vitev [12–15]. Our purpose here was simply to show that our model is also able to reproduce the $R_{AA}(p_T)$, which can be considered as the minimum requirement. However, our result shows also that at the level of $R_{AA}(p_T)$ both a realistic density profile like the WS or the SE profile can describe the data reasonably well. We have seen that the main reason behind the similar final result between the two different geometries, WS and SE, relies on the compensation between two effects. In fact, for SE one has a nonrealistic uniform density; however, the minijets are also distributed uniformly. So the uniform density profile on the one hand overestimates the amount of quenching close to the surface but on the other underestimates the one in the core of the fireball. In addition, in such a modeling the fact that minijets are uniformly distributed overestimates the amount of minijets leaving the fireball nearly unquenched. Even if one could suspect that a balance among these effects should not *a priori* hold at all centralities, our results show that the breaking of such a cancellation effects is small. Therefore by mean of the $R_{AA}(p_T)$ even the SE simplified modeling cannot be discarded. The same conclusion can be drawn looking also at the R_{AA} at $p_T > 6$ GeV as a function of centrality shown in Fig. 3. However, as expected, we see that surface effects leading to less suppression for a WS geometry are more important for a smaller $N_{\rm part}$.

Furthermore, if we consider a GLV formalism with a running coupling constant $\alpha_s(T)$, GLV-$\alpha_s(T)$, the $R_{AA}(p_T)$ is well reproduced at same level of quality. Hence, looking at $R_{AA}(p_T)$, one is not able to clearly discriminate the geometry or the temperature dependence of the quenching, even if one looks at the evolution with centrality. Therefore, in agreement with Refs. [32,33], we find that $R_{AA}(p_T)$ carries only a weak information on the jet quenching process, apart, of course, from the total amount of quenching, which in itself is of fundamental importance and has led to a first estimate of the average initial gluon density.

In the next section we investigate both the elliptic flow at high p_t and the flavor dependence of the quenching. In fact, both observables are still hardly accounted for quantitatevely by the present models.

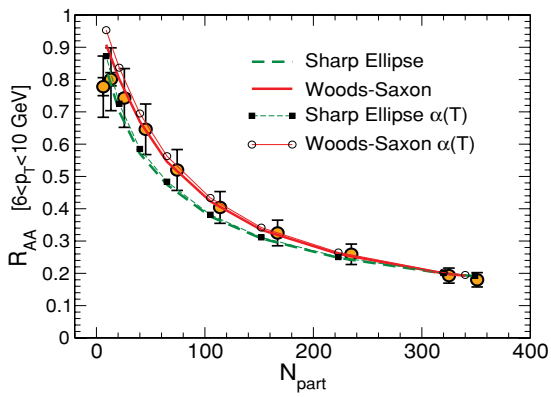

FIG. 3. (Color online) Nuclear modification factor as a function of the number of participants in Au + Au at 200 A GeV for two density profiles of the bulk matter: Glauber from WS nuclei profile (solid line) and SE shape (dashed line).

III. ANGULAR AND FLAVOR DEPENDENCE OF THE QUENCHING

The first analysis of jet suppression has shown that it is very difficult to have an agreement between models and experiments for the dependence of the R_{AA} on the azimuthal angle ϕ with respect to the reaction plane in noncentral collisions [33]. Such a dependence arises from the "almond" (elliptic) shape of the overlap region of two colliding nuclei. In particular, for large $p_t > 6$ GeV, where hard processes dominate [11], partons penetrating the fireball in different directions lose different amounts of energy according to their varying paths that on average are larger in the out-of-plane direction. A measure of this effect is provided by the second Fourier coefficient of the distribution, namely, the elliptic flow:

$$v_2(p_T) \equiv \frac{\int_0^{2\pi} d\phi \cos(2\phi)[d^2N/dp_t d\phi]}{\int_0^{2\pi} d\phi[d^2N/dp_t d\phi]}. \qquad (15)$$

Unexpectedly, measured $v_2(p_T)$ happened to be considerably larger than what jet quenching models predicted. It was noted in Ref. [34] that for very strong quenching only jets emitted from the surface of the almond shape can be observed and the data for $v_2(p_T)$ are very close to such a limiting case. However, generally, three other assumptions are made, namely, (i) quenching is proportional to matter density; (ii) colliding nuclei were approximated by homogeneous sharp-edged spheres; (iii) only the net rate of energy loss is considered discarding the emission-absorption processes that generally can lead to an enhancement of the collective flows [13]. Studies by Drees *et al.* [35] relaxed the second assumption, with realistic nuclear shapes, which only made contradiction with data even stronger. A result that is confirmed also by the present work.

We mainly explore the effect of the first assumption by exploring the four different kinds of energy loss shown in Fig. 1. In Fig. 4, we show the resulting v_2 for pions in Au + Au at $\sqrt{s_{NN}} = 200$ GeV and an impact pararameter $b = 7.5$ fm corresponding to a minimum bias condition for which the experimental value of elliptic flow is about 0.11 [36], as shown in the figure by hatched area. Such data correspond to the integrated value for $p_T > 6$ GeV.[1] We can see that even if the amount of total quenching has been fixed to the experimental value of $R_{AA}(p_T)$, the amount of elliptic flow is still strongly dependent on the temperature dependence of the $\Delta E_{\rm loss}$. Specifically, from the thin to the thick solid line, we see that v_2 increases if the $E_{\rm loss}$ is stronger as $T \to T_c$ (thick solid line in Fig. 1), which means later in the evolution of the QGP, except for the surface. In Fig. 5 the same quantity is plotted for the case of a bulk density given by the SE. Again we find that in agreement with other calculations [18,19], the elliptic flow is significantly larger if most of the energy loss takes place closer to T_c (thick solid line). If instead the energy loss take place mainly at high temperature and/or density (thin solid line) the v_2 is essentially vanishing. The dashed line is the result with the GLVc that represents a case in which the energy loss is

[1]We do not show the experimental data vs p_T owing to the present controversial issues related with their measurement.

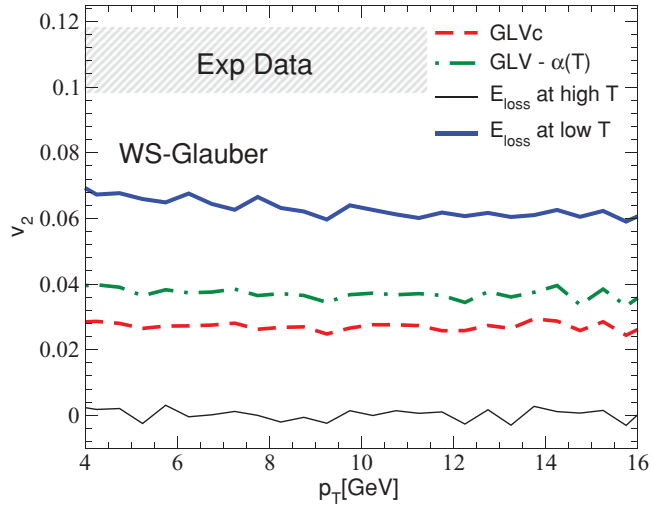

FIG. 4. (Color online) Elliptic flow for the pions coming from quark and gluon fragmentation for the different T dependence of the energy loss, as shown in Fig. 1. The density profile of the bulk is given by the Glauber model (see Sec. II).

essentially proportional to the density. The dot-dashed line is the GLV-$\alpha_s(T)$ that reweighs the temperature dependence through the coupling $\alpha_s(T)$, giving an estimate of the effect of asymptotic freedom. Such an effect is not negligible and for the SE geometry it seems to give already a v_2 very close to the much more extreme case represented by the thick solid line, that is, quenching dominated by the region close to T_c.

The correlation between the temperature dependence of ΔE and the amount of elliptic flow developed is clear. In fact, at variance with $R_{AA}(p_T)$ the v_2 has a longer formation time because the minijets have to explore the shape of the fireball. For example, if one considers the extreme case of a very strong quenching that takes place on distances much lower than the fireball size, then there would be no elliptic flow (like in the $E_{\rm loss}$ at high T case).

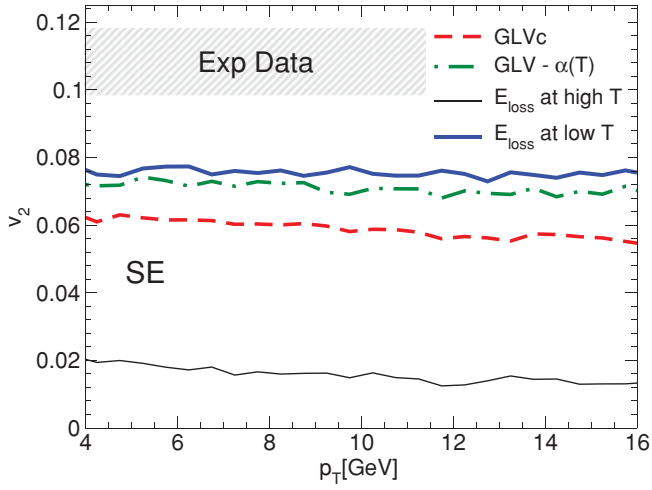

FIG. 5. (Color online) Elliptic flow for the pions coming from quark and gluon fragmentation for the different T dependence of the energy loss, as shown in Fig. 1. The bulk density profile is a sharp uniform elliptic shape.

It seems to be quite likely that experiments are telling us that quenching is likely to be *not* proportional to the matter entropy density or temperature, but a decreasing function of it. This is what is essentially discussed in Refs. [18,19], where, however, it was implicitely assumed that the amount of quenching of quarks and gluons is equal among them and to the hadronic one. Here we relax such assumptions, showing that the temperature (or entropy density) dependence of $\Delta E_{\rm loss}$ modifies not only the v_2 but also the relative amount of quenching of quarks and gluons. This does not meant to be just a more detailed calculation but is indeed related to another puzzle of the jet quenching phenomena observed more recently in the experimental study of the chemistry of the minijet suppression [37,38]. We discuss it in the next subsection.

A. Quark-to-gluon modification factor

The QCD owing to its SU(3) Lie algebra gives a factor $C_R = 9/4$ larger for the energy loss of gluons with respect to that of quarks. For this reason, sometimes it is implicitly assumed that the ratio between the suppression of the gluons $R_{AA}(g)$ and the suppression of quarks $R_{AA}(q)$ is such that $R_{AA}(q)/R_{AA}(g) = 9/4$. From this expectation one would think that the (anti-)protons are more suppressed with respect to pions because they come more from gluon fragmentation than from quark fragmentation with respect to pions. The data at RHIC, however, have shown that also for such an observable there is no agreement with the data. In fact, even outside the region where coalescence should be dominant [4,5] the protons and the antiprotons appear to be less suppressed than the pions and ρ^0 [37,38]. Again we can see that going beyond the simple amount of quenching given by $R_{AA}(p_T)$ neither the azimuthal dependence nor the flavor dependence of the quenching appear to be in agreement with the data. We call these open issues the "azimuthal" and the "flavor" puzzles, respectively. We show that even if R_{AA} for central collisions is fixed to be $\sim$0.2, the $R_{AA}(q)/R_{AA}(g)$ is affected by the temperature dependence of $\Delta E_{\rm loss}$.

In Fig. 6 we show the ratio of the $R_{AA}(q)/R_{AA}(g)$ for the WS geometry and the four different temperature dependencies of the energy loss $\Delta E_{\rm loss}$ as in Fig. 1. We can see that the standard GLVc energy loss does not give the expected ratio 9/4 for $R_{AA}(q)/R_{AA}(g)$ but a lower value around 1.8, which represents already a non-negligible deviation from 2.25. We can, however, see that if the energy loss would be strongly T-dependent and dominated by the $T \gtrsim T_c$ region $R_{AA}(q)/R_{AA}(g)$ can increase up to about 2.3 while, oppositely, if it is dominated by the high-temperature region (thin solid line) the $R_{AA}(q)/R_{AA}(g)$ can become as small as 1.5. However, our study of the elliptic flow, as well as previous studies, show that an energy loss that increase with T would generate a tiny v_2 very far from the observations. Such an effect is totally discarded in Refs. [18,19], which neglect the different quenching of quarks and gluons. In other words, while the indication of a $\Delta E(T)$ increasing as $T \to T_c$ is confirmed also by our model to reproduce experimental data for v_2, we notice this would lead to a larger $R_{AA}(q)/R_{AA}(g)$ ratio, increasing the disagreement with the $R_{AA}(p_T)$ observed for

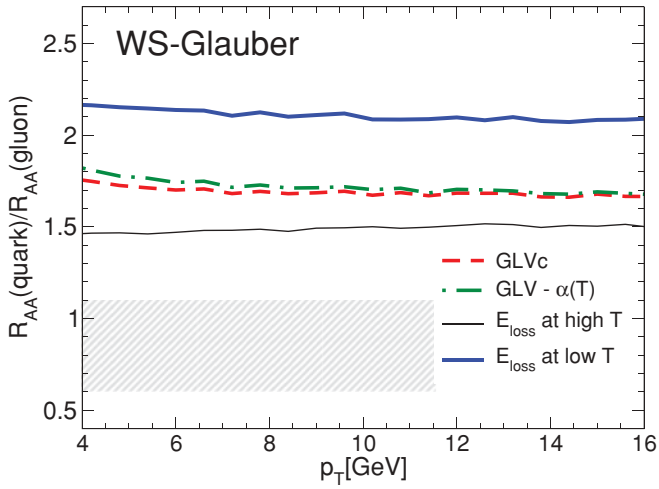

FIG. 6. (Color online) Ratio of quark to gluon R_{AA} for the different T dependence of the energy loss, as shown in Fig. 1. The short-dashed line corresponds to the 9/4 value. The density profile of the bulk is that given by the Glauber model. The shaded area shows approximatively the value expected for the ratio according to the experimental observations and using the AKK fragmentation function.

the various hadrons like p, $\bar{p}$, π that show the R_{AA} of baryons less suppressed respect to the pionic one. The shaded area in Figs. 6 and in 7 approximately shows the expected value for the ratio $R_{AA}(q)/R_{AA}(g)$ that can be inferred from the statistical and systematic uncertainties in the experimental data for R_{AA} of various hadrons. However, though significant uncertainties come from the fragmentation functions, our estimate is done using the AKK parametrization.

In this respect we notice also another potential problem that can arise for simplified fireball modeling when extreme $\Delta E(T)$ are considered and more exclusive observables are investigated. More explicitly, we refer to the SE fireball that

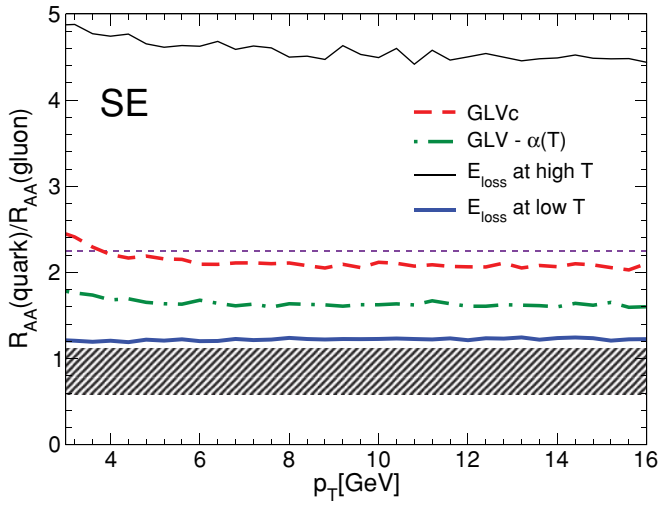

FIG. 7. (Color online) Ratio of quark to gluon R_{AA} for the different T dependence of the energy loss as shown in Fig. 1. The short-dashed line corresponds to the 9/4 value. The density profile of the bulk is that of a SE shape. The shaded area is as in Fig. 6.

neglects the surface of the fireball. In Fig. 7 we show that the results have an opposite pattern for the SE geometry with respect to the realistic WS one. The standard GLV energy loss gives approximately the expected ratio of 9/4 for $R_{AA}(q)/R_{AA}(g)$. This probably led to the association of the 9/4 factor on $E_{\rm loss}$ to that on $R_{AA}(q)/R_{AA}(g)$. However, this ratio is more sensitive to the temperature dependence of the energy loss in a way that is exactly opposed to what we have seen for the WS geometry. For this kind of geometry (SE), if the energy loss is stronger at high temperature, the $R_{AA}(q)/R_{AA}(g)$ can result to be almost 5 (thin solid line); however, if the enery loss is stronger closer to T_c the R_{AA} would be just slightly above 1 (thick solid line). This means that the ratio tends to decrease from 5 to 1 if the energy loss is dominated by the high temperatures ($T \to 2T_c$) or by the low ones ($T \sim T_c$).

It is instructive to explain the origin of such a strong effect of the density profile, but before we note that such an unexpected strong effect shows up only when extreme $\Delta E(T)$ are considered. In fact, the standard GLVc $E_{\rm loss}$ is modified by about a 15% moving from a WS-Glauber to a simple SE profile.

To understand the mechanism behind the determination of the ratio $R_{AA}(q)/R_{AA}(g)$, we discuss an oversimplified case in which all quarks lose the same amount of energy and all gluons lose their energy according to $\Delta E_g = 9/4\Delta E_q$. For such a simple case the spectra after quenching are shifted by a quantity equal to the lost energy. Quarks that finally emerge with an energy $E_f = p_T$ are those which before quenching had an energy $E_i = p_T + \Delta E$. So R_{AA} for quarks is equal to the ratio between the parton distributions in momentum-space without quenching $f(p_T)$ and the quenched one given by $f(p_T + \eta\Delta E)$, where $f(p_T) = dN/d^2p_T dy$ is given by Eq. (1), $\eta = 1$ for quarks and $\eta = 9/4$ for gluons. Therefore, the R_{AA} is

$$R_{AA}(p_T) = \frac{f(p_T + \eta\Delta E)}{f(p_T)}, \tag{16}$$

and the ratio between quark and gluon nuclear modification factors is

$$\frac{R_{AA}(q)}{R_{AA}(g)} = \frac{f_q(p_T + \Delta E)}{f_q(p_T)} \frac{f_g(p_T)}{f_g(p_T + (9/4)\Delta E)}. \tag{17}$$

Of course, there is no reason why this ratio must be 9/4 and we can also see that even without the 9/4 factor there can be a $R_{AA}(q)/R_{AA}(g)$ that is not one. In Fig. 8 is shown the dependence of the ratio on ΔE for partons with $p_T = 10$ GeV and we can see that $R_{AA}(q)/R_{AA}(g)$ quickly increases with ΔE even if the ratio of the quark-to-gluon energy loss is 9/4. The ratio is about 4 for a $\Delta E \sim 2$ GeV/fm. We see that this observation is fundamental to understanding the relation between $\Delta E_{\rm loss}$ and the ratio $R_{AA}(q)/R_{AA}(g)$. In this very simplified model, the $R_{AA}(q)/R_{AA}(g)$ would be very large for an average energy loss $\langle \Delta E_q \rangle = 4$ GeV typical of central collisions where $R_{AA}(p_T) \sim 0.2$. From Fig. 8 we can see that this would give a $R_{AA}(q)/R_{AA}(g) \sim 8$.

One can move toward a minimal realistic model distinguishing among partons two classes of particles: those that undergo a large quenching and those that lose no energy, or better, a

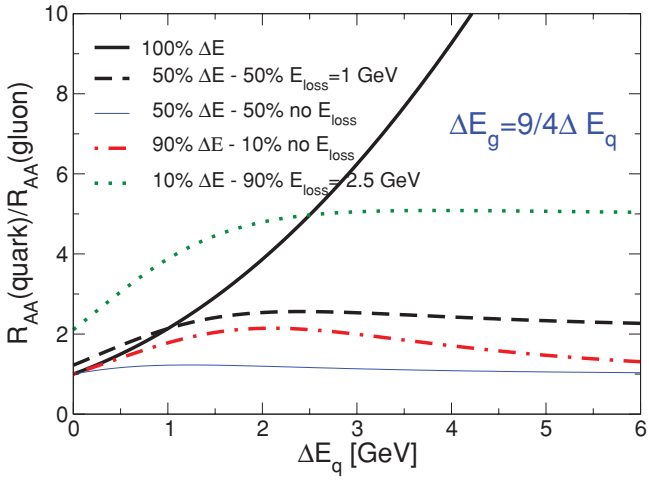

FIG. 8. (Color online) Ratio of quark to gluon R_{AA} as a function of the quark energy loss $\Delta E_q = 4/9\Delta E_g$ for different models of the jet quenching; see text for details.

small amount of energy, usually associated with the minijets generated at the surface. Let us consider a case in which 50% partons lose an energy $\Delta E_q = 1$ GeV $= 4/9\Delta E_g$, while the other 50% lose the energy ΔE_q indicated in Fig. 8. In such a case the evolution of $R_{AA}(q)/R_{AA}(g)$ is very different with respect to the first case as shown by the much milder increase of the dashed line that reaches a maximum of about 2.6 and even decrease for a $\Delta E_q > 2$ GeV.

This clearly indicates that because of the rapidly falling distribution with p_T, the determination of the ratio is dominated by those partons that suffer less energy loss. If, for example, 50% of the particles do not lose energy, then whatever the energy loss of the other partons is, the $R_{AA}(q)/R_{AA}(g)$ will be equal to one. This is shown by the thin solid line in Fig. 8. Indeed, already if only 10% of partons do not lose energy, the ratio stays below 9/4 regardless of the $E_{\rm loss}$ of the other 90% of particles and even decreases if those particles lose a large amount of energy, bringing the value again closer to one. This is shown by the dot-dashed line in Fig. 8, where one can realize the huge impact of the particles that do not lose energy comparing thick solid and dot-dashed lines, which differ only by the fact that 10% of the particles do not lose energy. Finally, with the dotted line in Fig. 8, we show a system in which most of the particles undergo a quenching with $\Delta E_q = 2.5$ GeV $= 4/9\Delta E_g$. This is closer to a case in which most of the particles undergo a similar strong quenching. In summary, we can say that the $R_{AA}(q)/R_{AA}(g)$ is not really directly linked to the relative amount of quark and gluon energy loss because it is largely affected by the way the energy loss is distributed among partons. In particular, once there are minijets that do not suffer energy loss, the ratio $R_{AA}(q)/R_{AA}(g)$ gets closer to one, because it is more affected by these minijets. Hence, a careful treatment of the corona effect also would much likely give a significant contribution to the determination of the $R_{AA}(q)/R_{AA}(g)$.

On the basis of the preceding discussion, it is possible to understand the dependence of $R_{AA}(q)/R_{AA}(g)$ on the temperature dependence $\Delta E(T)$, seen in Figs. 6 and 7 and its opposite behavior between the WS and SE geometries for the density profile. In the case of energy loss at low temperature with a SE profile, the quenching happens at the end of the lifetime of the fireball because there is a direct relation between time and temperature [see Eq. (12)]. Therefore, in the case of the energy loss increasing as $T \to T_c$ many particles escape without losing energy in the SE profile. Only the particles in the inner part of the fireball are quenched. This means that we are closer to the schematic case described by the thin solid line for large ΔE in Fig. 8. Most particles do not lose energy, the rest lose a large amount of energy, and in fact $R_{AA}(q)/R_{AA}(g)$ is close to one (see Fig. 7).

Instead, if the quenching is larger at high temperature, all particles lose energy early and, except for those very close to the surface, most of particles $\Delta E \gtrsim 2.5$ GeV. In this case, there are essentially no particles that do not lose energy. So we are closer to the case described by the dotted line for which $R_{AA}(q)/R_{AA}(g)$ is about 5, compared to thin solid line of Fig. 7.

In the case of WS geometry, in general, there is no direct relation between time and temperature because on the surface one will have already at early times a low temperature. Therefore, in this case an energy loss dominated by high temperatures means that the quenching is large only on the inner part of the fireball while particles in the surface lose a small amount of energy. We are close to the case described by the dot-dashed line in Fig. 8, and the $R_{AA}(q)/R_{AA}(g)$ is in fact about 1.5. It is difficult to reach one because owing to the density profile anyway all the particles lose at least some finite energy. Instead, if the quenching takes place mainly at low temperature ($T \to T_c$), this means that energy loss is strong in a layer on the surface of the fireball, and because all particles must go through this layer at some time, all of them lose a large amount of energy. We understand that this is very different, essentially the opposite, with respect to the SE case. In the latter case a $\Delta E(T)$ with a maximum at $T \to T_c$ means that most of the particles escape owing to the direct time-temperature relation that is not dependent on space. For WS-Glauber profile, such a case means just the opposite; that is, all the particles lose a similar amount of energy. This is essentially the reason underlying the opposite trend seen in Figs. 6 and 7. We finally notice that the importance of such details emerges only if extreme energy losses in T-dependence are considered.

The conclusion of this study is twofold:

(i) If one tries to reproduce the large value of elliptic flow using a type of energy loss that increases with decreasing temperature, there is a simultaneous increase of the $R_{AA}(q)/R_{AA}(g)$ enhancing the discrepancy with respect to the observed "flavor" dependence of the suppression that seems to prefer a ratio close to or even smaller than one [37].

(ii) When peculiar energy dependencies are considered, the specific density-temperature profile can become very important for a quantitative evaluation of the observables.

These results lead us to make two important observations: (i) The SE profile is able to describe the observed $R_{AA}(p_T)$,

but it is inadequate to reproduce the ratio $R_{AA}(q)/R_{AA}(g)$, and furthermore, it cannot be used even for a qualitative analysis of this ratio because it gives opposite results to the more realistic WS profile. (ii) In Figs. 4 and 5 we show that an enhancement of the energy loss near T_c increases the elliptic flow toward an agreement with the experimental data. However, such a $\Delta E(T)$ is associated with an enhancement of $R_{AA}(q)/R_{AA}(g)$, in apparent disagreement with the data [38].

IV. CORRELATION BETWEEN $R_{AA}(q)/R_{AA}(g)$ AND ELLIPTIC FLOW

To solve what we have called the flavor puzzle, inelastic collisions that cause a change of the flavor have been invoked [20–23]. Such a process would in the end produce a net conversion of quarks into gluons, hence, a decrease of gluon suppression with respect to the direct suppression and an increase of the quark one [20]. In Ref. [20] the conversion rate of a quark jet to a gluon jet and vice versa owing to two-body scatterings has been calculated. An enhancement factor $K_c = 4$–6 that accounts for nonperturbative effect is needed to produce a nearly equal suppression of quarks and gluons. This is not an unreasonable enhancement factor considering that at our energy a $K \sim 4$ is necessary also to have the right minijet initial distributions in pp if one starts from a simple second-order pQCD calculation. We have included the flavor conversion mechanism in our code in a fashion similar to Ref. [20]. To check our code and to have a direct link to the previous calculations of Fries, Ko, and Liu, we have used the same density profile (i.e., a SE profile), same conversion rate, and $\Delta E_{\rm loss}$ derived by them at leading order in the pQCD expansion.

In Fig. 9 we show $R_{AA}(q)/R_{AA}(g)$ for different values of K_c. Notice that with the $\Delta E_{\rm loss}$ of Ref. [20] the ratio $R_{AA}(q)/R_{AA}(g)$ without conversion is again different and moreover quite larger than 9/4. However, a $K_c \sim 4$–6 is able to reduce that ratio by about a factor of three, making it close

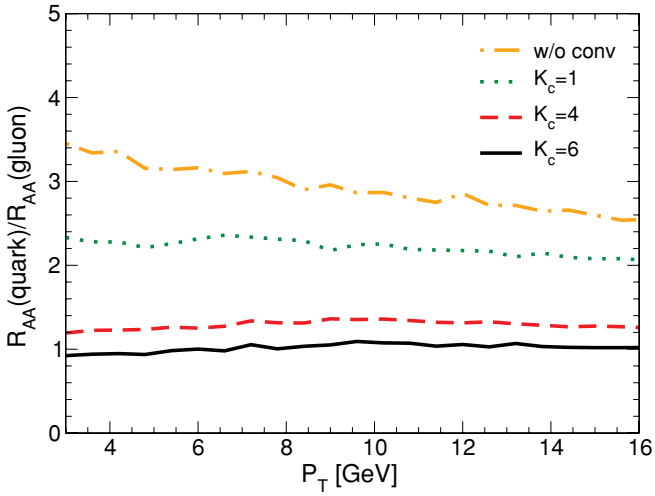

FIG. 9. (Color online) Ratio of quark to gluon in Au + Au collisions ($b = 7$ fm) for the energy loss derived in Ref. [20] with different factors upscaling the pQCD conversion rate.

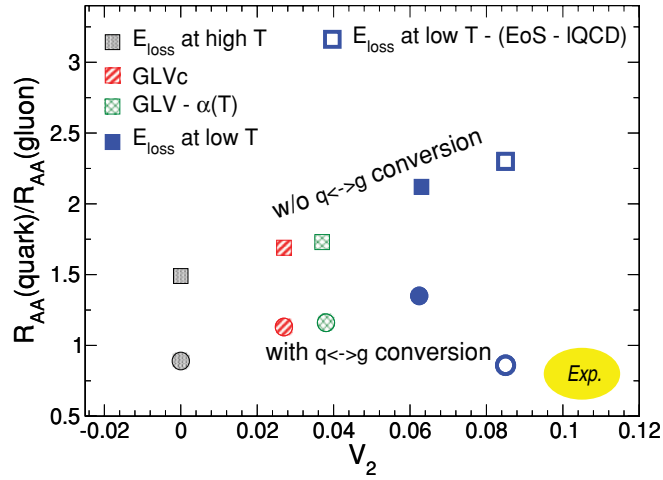

FIG. 10. (Color online) Correlation between the $R_{AA}(q)/R_{AA}(g)$ and the elliptic flow of pions ($6 < p_T < 10$ GeV) for a WS density profile. The squares refer to calculation without jet conversion, while the circles are results including jet conversion with a $K_c = 6$ factor.

to unity. After this test we have fixed $K_c = 6$ and performed the calculation with the four different energy losses, as shown in Fig. 1. In Fig. 10 we show directly the $[R_{AA}(q)/R_{AA}(g), v_2]$ plot. This plot manifests a clear but nontrivial correlation between $R_{AA}(q)/R_{AA}(g)$ and the v_2. The upper symbols are the results without the jet flavor conversion and we can see that such a correlation drives the data far from the experimental observed values of a $v_2 \sim 0.1$ and an $R_{AA}(q)/R_{AA}(g) \leqslant 1$ [to account for the $R_{AA}(p + \bar{p}) > R_{AA}(\pi^+ + \pi^-)$ with AKK fragmentation function]. The lower symbols correspond to the results including the rate of inelastic collisions and we can see that this process allows to get closer to the experimental region because they change the $R_{AA}(q)/R_{AA}(g)$ without modifying the elliptic flow of pions. Figure 10 essentially demonstrates that if one tries to reproduce simultaneously the $R_{AA}(p_T)$ and v_2 and $R_{AA}(q)/R_{AA}(g)$, a $\Delta E(T)$ increasing as $T \to T_c$ is needed but also that in such a case a flavor-conversion process becomes even more necessary.

However, at this point a quantitative study should be performed, employing a more accurate dynamics for the bulk evolution given by hydrodynamics or partonic transport theory that includes three-body radiative processes [39,40]. In fact, especially if more peculiar energy loss dependence has to be investigated, it is important to have a quite realistic density and energy-density profile, as we have discussed earlier. Furthermore, fluctuations in the energy loss [10,41], the gain-loss processes [13], and the elastic energy loss [42,43] should be included because they can give correction to both $R_{AA}(p_T)$ and v_2.

V. IMPACT OF THE EQUATION OF STATE

As a last point, we explored the impact of the EoS on the observables and especially the correlation between $R_{AA}(q)/R_{AA}(g)$ and $v_2(p_T)$. This has to be taken as a first explorative study.

We notice that even if the free gas approximation is a quite reasonable approximation for describing the relation between density and temperature for most of the evolution of the expanding QGP, it is not true close to T_c, where the relation between temperature and density is strongly modified by the crossover phase transition. One generally thinks that for the description of the high-p_T particles this can be discarded in the first approximation. However, once it is opened the way to the possibility of a quenching that is not proportional to the density but is stronger close to the phase transition, we will show that one should more carefully look into the problem. In fact, if quenching would be dominated by the $T \to T_c$ region, the time spent in this region by the fireball can be strongly modified if a realistic EoS is considered. In fact, for a simple 1 + 1D expansion, the relation between temperature and density is modified from Eq. (12) to

$$\frac{T}{T_0} = \left(\frac{\rho}{\rho_0}\right)^{\beta(T)} = \left(\frac{\tau_0}{\tau}\right)^{\beta(T)}, \tag{18}$$

where $\beta(T)$ is a temperature-dependent coefficient that can be obtained from a fit to lQCD data [44]. We have found

$$\beta(T) = \frac{1}{3} - a\left(\frac{T_c}{T}\right)^n, \quad T \geqslant T_c, \tag{19}$$

with $a = 0.15$ and $n = 1.89$, and of course for $T \gg T_c$ one gets $\beta \sim 1/3$. The parameters have been calculated from a fit to the lQCD data of Ref. [44] on the energy density and pressure. We see that close to T_c the β coefficient is quite small, which means that even if the density goes down as τ^{-1}, the temperature stays nearly constant, as one can expect in a first-order or strong crossover phase transition. This means that the system spends more time close to T_c with the simple picture given by Eq. (12) usually assumed.

To estimate the impact of this correction, we have performed a simulation for the $\Delta E_{\rm loss}(T)$ behavior represented by the thick solid line in Fig. 1, which is similar to the delayed energy loss proposed by Pantuev [19] as a solution for the observed large elliptic flow. We consider only this case because it is, of course, the one that is much more affected by the modification implied by Eq. (18). Instead, for the opposite case of an $E_{\rm loss}$ dominated by the high T the effect is vanishing. We have again taken care to regulate the total energy loss to have the correct amount of $R_{AA}(p_T)$.

The results are given by open symbols in Fig. 10. The open square is the result without the inclusion of the flavor conversion mechanism and shows a further increase of both v_2 and $R_{AA}(q)/R_{AA}(g)$, in line with the previously seen correlation. The enhancement of the v_2 in itself is attributable to the fact that with an EoS the system spends more time close to T_c; therefore, to have the same amount of suppression, most of the energy loss occurs later. However, more interestingly, the inclusion of the $q \leftrightarrow g$ conversion results in greater efficiency than in the previous case, generating a strong decrease in $R_{AA}(q)/R_{AA}(g)$ while keeping the same v_2. The stronger effect of flavor conversion is again attributable to the longer lifetime. The final result is a combination that moves the final value of both v_2 and $R_{AA}(q)/R_{AA}(g)$ much closer to the experimental ones [36] shown by the shaded area in Fig. 10. We also notice that a $R_{AA}(q)/R_{AA}(g) < 1$ is obtained, while generally it is believed that flavor conversion by inelastic collisions can give at most $R_{AA}(q)/R_{AA}(g) = 1$ [37].

This last result about the impact of a realistic EoS deserves a more careful treatment, again employing a more realistic description of the bulk. Indeed, a full description of the dynamics related to the crossover region should include also the gradual change from a quark-gluon plasma to a hadronic gas. However, this would be outside our goal for the present work.

VI. CONCLUSIONS

In the present work we have considered different temperature dependencies of the energy loss, tuning always the parameters to reproduce the experimentally $R_{AA}(p_T)$ suppressions of pions. We have shown that even if the $R_{AA}(p_T)$ is fixed, different $\Delta E(T)$ generate very different values for both the v_2 and the $R_{AA}(q)/R_{AA}(g)$. Indeed, both quantities are quite puzzling because standard jet quenching models are not able to reproduce any of them. We referred to this as the azimuthal and flavor puzzle. We have found, however, that there is a correlation between these two observables that is determined by the temperature (or density) dependence of the quenching. In agreement with Refs. [18,19], we have found that if the quenching is dominant closer to T_c, the v_2 is enhanced getting closer to the data. However, while in Refs. [18,19] it is discarded as a separate treatment of quark and gluons, their $E_{\rm loss}$ leads to a quite large ratio $R_{AA}(q)/R_{AA}(g)$, which would be incompatible with the observed systematics of $R_{AA}(p + \bar{p}) > R_{AA}(\pi^+ + \pi^-) \sim R_{AA}(\rho^0)$. It appears that while the v_2 would suggest a $\Delta E(T)$ that increases toward T_c, the $R_{AA}(q)/R_{AA}(g)$ would become too large even if we do not yet have a direct measurement of $R_{AA}(q)/R_{AA}(g)$ and we impinge on the uncertainties coming from the fragmentation functions.

In this context we have also noticed an unexpected strong dependence on the density profile of the fireball that emerges for extreme choices of $\Delta E(T)$, while the dependence is milder but not negligible for more standard energy loss like the GLV one. This puts a warning for further studies: Once going beyond the simple $R_{AA}(p_T)$ factor, one has to rely on a realistic dynamical evolution of the bulk matter like those supplied by hydrodynamics and/or parton cascades [39].

It seems that the only way to get closer to the observed values for $R_{AA}(p_T)$, v_2, and $R_{AA}(q)/R_{AA}(g)$ solving both the azimuthal and flavor puzzles, is to have both $\Delta E(T)$ increasing close to T_c and a flavor-conversion mechanism. Finally, we point out that while generally the free gas approximation is quite reasonable to describe the expansion of the QGP fireball, this is no longer true if the energy loss occurs dominantly close to T_c. In such a case it has a significant impact to take into account the strong deviation from the free gas approximation occurring in the crossover region and leading to a slowing down of the cooling close to T_c. This increases further the time spent around T_c, which enhances both v_2 and the efficiency of the $q \leftrightarrow g$ in medium conversion, moving the values of $[R_{AA}(q)/R_{AA}(g), v_2]$ close to the observed ones.

It is of course important to study how the longer lifetime and higher temperatures reached at LHC energies

affect the observed correlations. Furthermore, in Ref. [24] it has been pointed out that a better probe of the flavor-conversion mechanism is supplied by a high p_T strangeness enhancement. It remains to be studied if such an enhancement is affected by the T dependence of the energy loss.

In summary, we have pointed out the impact of peculiar T dependencies of the $E_{\rm loss}$ on both v_2 and $R_{AA}(q)/R_{AA}(g)$ and their correlation. Moreover, we have noticed the relevance that the EoS may have in case of $E_{\rm loss}$ dominated by the $T \to T_c$ region. In any case, our study, although already revealing several interesting indications, is mainly explorative. A more quantitative analysis should be performed with more sophisticated models that include the energy loss fluctuations, realistic gain and loss processes, elastic energy loss, and a more accurate description of the bulk.

[1] J. Adams *et al.*, Nucl. Phys. A **757**, 102 (2005); K. Adcox *et al.*, *ibid.* **757**, 184 (2005).
[2] P. Romatschke and U. Romatschke, Phys. Rev. Lett. **99**, 172301 (2007).
[3] U. W. Heinz, J. S. Moreland, and H. Song, Phys. Rev. C **80**, 061901 (2009).
[4] R. J. Fries, V. Greco, and P. Sorensen, Annu. Rev. Nucl. Part. Sci. **58**, 177 (2008).
[5] V. Greco, Eur. Phys. J. ST **155**, 45 (2008); V. Greco, C. M. Ko, and P. Levai, Phys. Rev. Lett. **90**, 202302 (2003); Phys. Rev. C **68**, 034904 (2003).
[6] J. D. Bjorken, FERMILAB-PUB-82-059-THY.
[7] D. A. Appel, Phys. Rev. D **33**, 717 (1986); J. P. Blaizot and L. D. McLerran, *ibid.* **34**, 2739 (1986).
[8] M. Gyulassy and M. Plumer, Phys. Lett. B **243**, 432 (1990); X. N. Wang and M. Gyulassy, Phys. Rev. Lett. **68**, 1480 (1992).
[9] R. Baier, Y. L. Dokshitzer, A. H. Mueller, S. Peigne, and D. Schiff, Nucl. Phys. B **484**, 265 (1997).
[10] M. Gyulassy, I. Vitev, X. N. Wang, and B. W. Zhang, in *Quark Gluon Plasma 3*, edited by R. C. Hwa and X. N. Wang (World Scientific, Singapore), pp. 123–191; X. N. Wang, Nucl. Phys. A **750**, 98 (2005); J. Casalderrey-Solana and C. A. Salgado, Acta Phys. Pol. B **38**, 3731 (2007).
[11] S. S. Adler *et al.* (PHENIX Collaboration), Phys. Rev. C **76**, 034904 (2007).
[12] M. Djordjevic and M. Gyulassy, Nucl. Phys. A **733**, 265 (2004).
[13] P. Arnold, G. D. Moore, and L. G. Yaffe, J. High Energy Phys. 06 (2002) 030; S. Turbide, C. Gale, S. Jeon, and G. D. Moore, Phys. Rev. C **72**, 014906 (2005).
[14] R. Baier, Y. L. Dokshitzer, A. H. Muller, S. Peigne, and D. Schiff, Nucl. Phys. B **483**, 291 (1997).
[15] N. Armesto, C. A. Salgado, and U. A. Wiedmann, Phys. Rev. D **69**, 114003 (2004).
[16] X. F. Guo and X. N. Wang, Phys. Rev. Lett. **85**, 3591 (2000).
[17] A. Majumder, E. Wang, and X. N. Wang, Phys. Rev. Lett. **99**, 152301 (2007).
[18] J. Liao and E. Shuryak, Phys. Rev. Lett. **102**, 202302 (2009).
[19] V. S. Pantuev, JETP Lett. **85**, 104 (2007).
[20] W. Liu, C. M. Ko, and B. W. Zhang, Phys. Rev. C **75**, 051901 (2007).
[21] W. Liu, C. M. Ko, and B. W. Zhang, Int. J. Mod. Phys. E **16**, 1930 (2007).
[22] W. Liu and R. J. Fries, Phys. Rev. C **77**, 054902 (2008).
[23] W. Liu and R. J. Fries, Phys. Rev. C **78**, 037902 (2008).
[24] R. J. Fries and W. Liu, Nucl. Phys. A **830**, 693C (2009).
[25] M. L. Miller, K. Reygers, S. J. Sanders, and P. Steinberg, Annu. Rev. Nucl. Part. Sci. **57**, 205 (2007).
[26] D. Kharzeev and M. Nardi, Phys. Lett. B **507**, 121 (2001).
[27] M. Gyulassy, I. Vitev, and X. N. Wang, Phys. Rev. Lett. **86**, 2537 (2001).
[28] A. Peshier, J. Phys. G **35**, 044028 (2008).
[29] P. F. Kolb and U. W. Heinz, in *Quark Gluon Plasma 3*, edited by R. C. Hwa and X. N. Wang (World Scientific, Singapore, 2004), p. 634.
[30] G. Ferini, M. Colonna, M. Di Toro, and V. Greco, Phys. Lett. B **670**, 325 (2009); S. Plumari, V. Baran, M. Di Toro, G. Ferini, and V. Greco, *ibid.* **689**, 18 (2010).
[31] M. Gyulassy, P. Levai, and I. Vitev, Phys. Lett. B **538**, 282 (2002).
[32] T. Renk, Phys. Rev. C **77**, 017901 (2008).
[33] S. A. Bass, C. Gale, A. Majumder, C. Nonaka, G. Y. Qin, T. Renk, and J. Ruppert, Phys. Rev. C **79**, 024901 (2009).
[34] E. V. Shuryak, Phys. Rev. C **66**, 027902 (2002).
[35] A. Drees, H. Feng, and J. Jia, Phys. Rev. C **71**, 034909 (2005).
[36] S. S. Adler *et al.* (PHENIX Collaboration), Phys. Rev. C **76**, 034904 (2007); A. Adare *et al.* (PHENIX Collaboration), Phys. Rev. Lett. **101**, 232301 (2008); J. Adams *et al.* (STAR Collaboration), *ibid.* **93**, 252301 (2004).
[37] A. Sickles, Nucl. Phys. A **830**, 131c (2009).
[38] Y. Xu *et al.*, Nucl. Phys. A **830**, 701c (2009); Y. Xu, J. Phys. G **37**, 094059 (2010); L. Ruan, *ibid.* **37**, 094013 (2010).
[39] O. Fochler, Zhe Xu, and C. Greiner, Phys. Rev. C **82**, 024907 (2010).
[40] Z. Xu and C. Greiner, Phys. Rev. C **71**, 064901 (2005).
[41] S. Wicks, W. Horowitz, M. Djordjevic, and M. Gyulassy, Nucl. Phys. A **784**, 426 (2007).
[42] G. Y. Qin, J. Ruppert, C. Gale, S. Jeon, G. D. Moore, and M. G. Mustafa, Phys. Rev. Lett. **100**, 072301 (2008).
[43] J. Auvinen, K. J. Eskola, and T. Renk, Phys. Rev. C **82**, 024906 (2010).
[44] F. Karsch *et al.*, Nucl. Phys. A **698**, 199 (2002); S. D. Katz, *ibid.* **774**, 159 (2006).